Ceramics International **24** (1998) 313–326

PII: S0272-8842(97)00017-5
0272-8842/98 $19.00+.00

Microstructure, Mechanical Properties and Thermal Shock Behaviour of Al_2O_3+ZrO_2+SiCw Composites

G. Y. Lin
Institute of Materials Science and Engineering, South China University of Technology, Guangzhou 510641, People's Republic of China

T. C. Lei
School of Materials Science and Engineering, Harbin Institute of Technology, Harbin 150001, People's Republic of China

(Received 1 July 1996; accepted 3 December 1996)

Abstract: The strengthening and toughening effects and mechanisms of combining both whisker reinforcing and zirconia phase transformation toughening in the Al_2O_3 matrix were systematically investigated in this paper. TEM observations showed that most of the SiCw/Al_2O_3 and SiCw/ZrO_2(2Y) interfaces are bonded tightly and there are no distinct second phases or intermediate layers formed at the interfaces. The addition of SiCw or ZrO_2(2Y) particles evidently improve the mechanical properties of Al_2O_3 ceramics and the more obvious strengthening and toughening effects can be obtained by adding both SiCw and ZrO_2(2Y) particles simultaneously to the Al_2O_3 matrix. The main toughening mechanisms in the Al_2O_3 + ZrO_2 + SiCw composites are whisker bridging and pull-out, crack deflection as well as dynamic t–m phase transformation toughening and microcrack toughening. The toughening effects of both SiCw and ZrO_2(2Y) particles are shown to be additive, but the addition of ZrO_2(2Y) particles decreases the strengthening effect of SiCw. The addition of SiCw can obviously improve the thermal shock resistance of Al_2O_3 and Al_2O_3 + ZrO_2(2Y) ceramics and the thermal shock resistance of Al_2O_3 + SiCw composites can be further improved by adding a few of ZrO_2(2Y) particles (10 vol%).

1 INTRODUCTION

ZrO_2 phase transformation toughening and whisker reinforcing have been proved to be two of the most effective methods for improving the mechanical properties of ceramics, which increase the strength and toughness of the ceramic matrices twofold or more.[1–4] ZrO_2 phase transformation toughening is mainly due to the tetragonal(t)–monoclinic(m) ZrO_2 phase transformation caused by the external stress which absorbs the fracture energy so that the stress concentration in the crack tip is released. But this toughening effect is limited by the temperature. It will disappear beyond the phase transformation temperature.[5] The whisker reinforcing is realised by the crack deflection, whisker pull-out and whisker bridging effects so that it is not sensitive to the temperature and this toughening effect can be held to a rather high temperature.[6] It will be of theoretical and practical importance to use these two toughening components to improve the mechanical properties of Al_2O_3 ceramics which is cheaper and widely used.

However, the experimental results show serious variations due to the differences in preparation of the materials or in the testing procedures. For example, Becher and co-workers[3,7,8] have shown that an addition of 20 vol% SiC whiskers (SiCw) to Al_2O_3 can increase the flexure strength and the fracture toughness from 400 MPa and 4.5 MPa$\sqrt{m}$ of the matrix to 650 MPa and 8.5 MPa$\sqrt{m}$ of the composite. A further addition of 20 vol% ZrO_2 to

the Al_2O_3 + 20 vol% SiCw increases the flexure strength to 750 MPa but decreases the fracture toughness slightly to 7.8 MPa$\sqrt{m}$. Claussen *et al.*[9,10] have shown that the composite of Al_2O_3 + 15 vol% t-ZrO_2 + 20 vol% SiCw aged at 1500°C for 24 h, has a flexure strength of 700 MPa and a fracture toughness of 13.5 MPa$\sqrt{m}$, but a hot-pressed composite of Al_2O_3 + 32 vol% m-ZrO_2 + 20 vol% SiCw has a flexure strength of 673 MPa and a fracture toughness of 6.3 MPa$\sqrt{m}$. Such variations in results have also been obtained by other authors.[11–13] Therefore, a systematic study of the strengthening and toughening effects of both SiCw and the ZrO_2 component on the Al_2O_3 matrix and, especially, to examine the combined effect of these two factors appear to be necessary.

2 EXPERIMENTAL PROCEDURE

The starting materials selected for investigation were α-Al_2O_3 powders with a grain size of 0.05 μm, ZrO_2–2 mol% Y_2O_3(ZrO_2(2Y)) powders with a particle size of 0.65 μm (having 34% t-ZrO_2 and 66% m-ZrO_2) and TWS-400 type of β-SiC whiskers of 1.0–1.4 μm in diameter and 20–30 μm in length (supplied by Japan Tokai Carbon Co.). The powders and the whiskers were mixed according to the compositions shown in Table 1, then inserted into plastic bottle together with ZrO_2 balls and absolute alcohol. The mixtures were then ground for 24 h and after drying were cold pressed at 200 MPa. The cold-pressed billets were then hot pressed under nitrogen at 1650°C and 25 MPa for 1 h to a size of 60×60×6 mm.

The hot-pressed billets were cut into specimens 3×4×36 mm for three-point bending tests to determine the flexure strength with a span of 30 mm, and a crosshead speed of 0.5 mm min^{-1}, the tensile surfaces were polished with 6~1 μm diamond paste. The residual strength of the composites after thermal shocking were determined at room temperature by using the specimens which were heated at a speed of 8~10°C min^{-1} to the predicted temperature and held for 30 min in a box-furnace, then dropped into the boiling water. Specimens for single-edge notched beam (SENB) tests, 2.5×5×25 mm, were cut for fracture toughness measurement with S/W = 4, a/W = 0.5. The width of the notch was 0.24~0.26 mm and a crosshead speed of 0.05 mm min^{-1} was used. Average values for six specimens were taken for both flexure strength and fracture toughness tests. All tests were performed on an Instron-1186 machine. The elastic modulus was determined by measuring the strains in the three-point bending tests and the hardness values obtained by using a Vicker's tester at a load of 20 kg. The density of the specimens were determined by the Archimede's method. A Hitachi S-570 type of scanning electron microscope and A CM-12 type of transmission electron microscope were used for examining the fracture morphology and microstructure of the specimens. A D/max-rB type of X-ray diffractometer was used for the structural analysis of the ZrO_2 component in the composites.

3 RESULTS AND DISCUSSION

3.1 Microstructure

The relative density (measured density divided by calculated theoretical density) values of the AS(Al_2O_3 + SiCw), AZS(Al_2O_3 + 20 vol% ZrO_2(2Y) + SiCw) and ASZ(Al_2O_3 + 20 vol% SiCw + ZrO_2 (2Y)) series of specimens are shown in Fig. 1. It is seen that the addition of SiCw slightly decreases the relative density of the Al_2O_3 matrix due to the geometric incompatibility of these two particles. However, due to the relatively long time of mixing the agglomeration of the Al_2O_3 grains and the networks of SiCw are satisfactorily avoided (as shown in Fig. 2) so that the relative density is at least 98.8% for Al_2O_3 + 30 vol% SiCw. The addition of ZrO_2–2 mol% Y_2O_3 (no more than 20 vol%) can further improve the densification of the composites. The relative density of ASZ3(Al_2O_3 + 20 vol% SiCw + 30 vol% ZrO_2(2Y)) composite is slightly lower than that of AS2(Al_2O_3 + 20 vol% SiCw) composite. This may be because the hot-pressing temperature of 1650°C is little higher for the ZrO_2 ceramics.[14]

The TEM photographs of the microstructure of Al_2O_3 + ZrO_2 + SiCw composites are shown in Figs 2 and 3. The white short rod microstructure is SiCw, dark particles are ZrO_2 grains, white particles

Table 1. Compositions of Al_2O_3+ZrO_2+SiCw composites

	Composites series AS(Al_2O_3+SiCw)				AZS(Al_2O_3+ZrO_2+SiCw)				ASZ(Al_2O_3+SiCw+ZrO_2)			
Content	AS0	AS1	AS2	AS3	AZS0	AZS1	AZS2	AZS3	ASZ0	ASZ1	ASZ2	ASZ3
Al_2O_3(vol%)	100	90	80	70	80	70	60	50	80	70	60	50
ZrO_2(vol%)	0	0	0	0	20	20	20	20	0	10	20	30
SiCw(vol%)	0	10	20	30	0	10	20	30	20	20	20	20

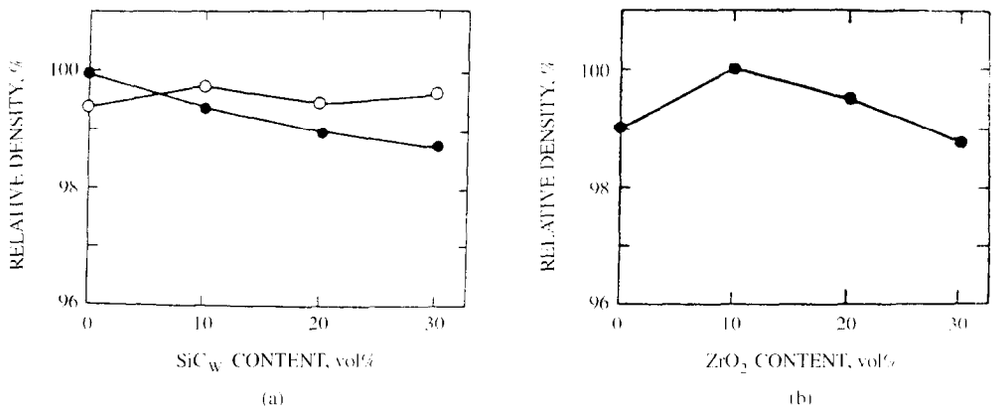

Fig. 1. Relative density of AS, AZS and ASZ composites as functions of toughening phase content. (a) ● AS(Al_2O_3 + SiCw), ○ AZS(Al_2O_3 + 20 vol% ZrO_2(2Y) + SiCw); (b) ASZ(Al_2O_3 + 20 vol% SiCw + ZrO_2(2Y)).

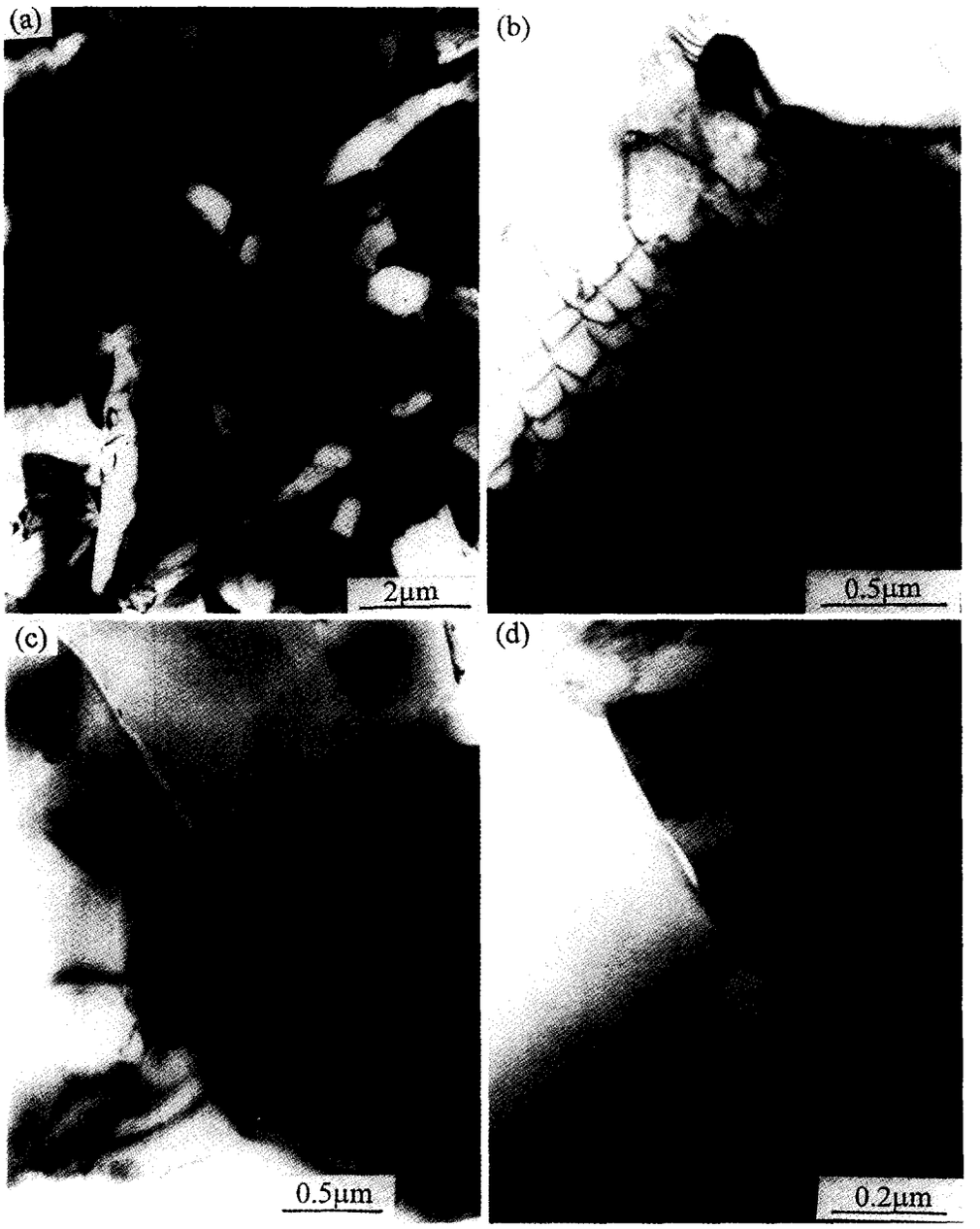

Fig. 2. TEM photographs showing the distribution of SiCw and ZrO_2(2Y) particles in $Al_2O_3 + ZrO_2$ + SiCw composites. (a), (b), (d) ASZ3 (Al_2O_3 + 20 vol% SiCw + 30 vol% ZrO_2(2Y)); (c) AZS2(Al_2O_3 + 20 vol% ZrO_2(2Y) + 20 vol% SiCw); (b), (c), also showing the dislocations in Al_2O_3 grains and (c), (d) showing the microcracks in the Al_2O_3 grain boundaries caused by the addition of ZrO_2(2Y) particles.

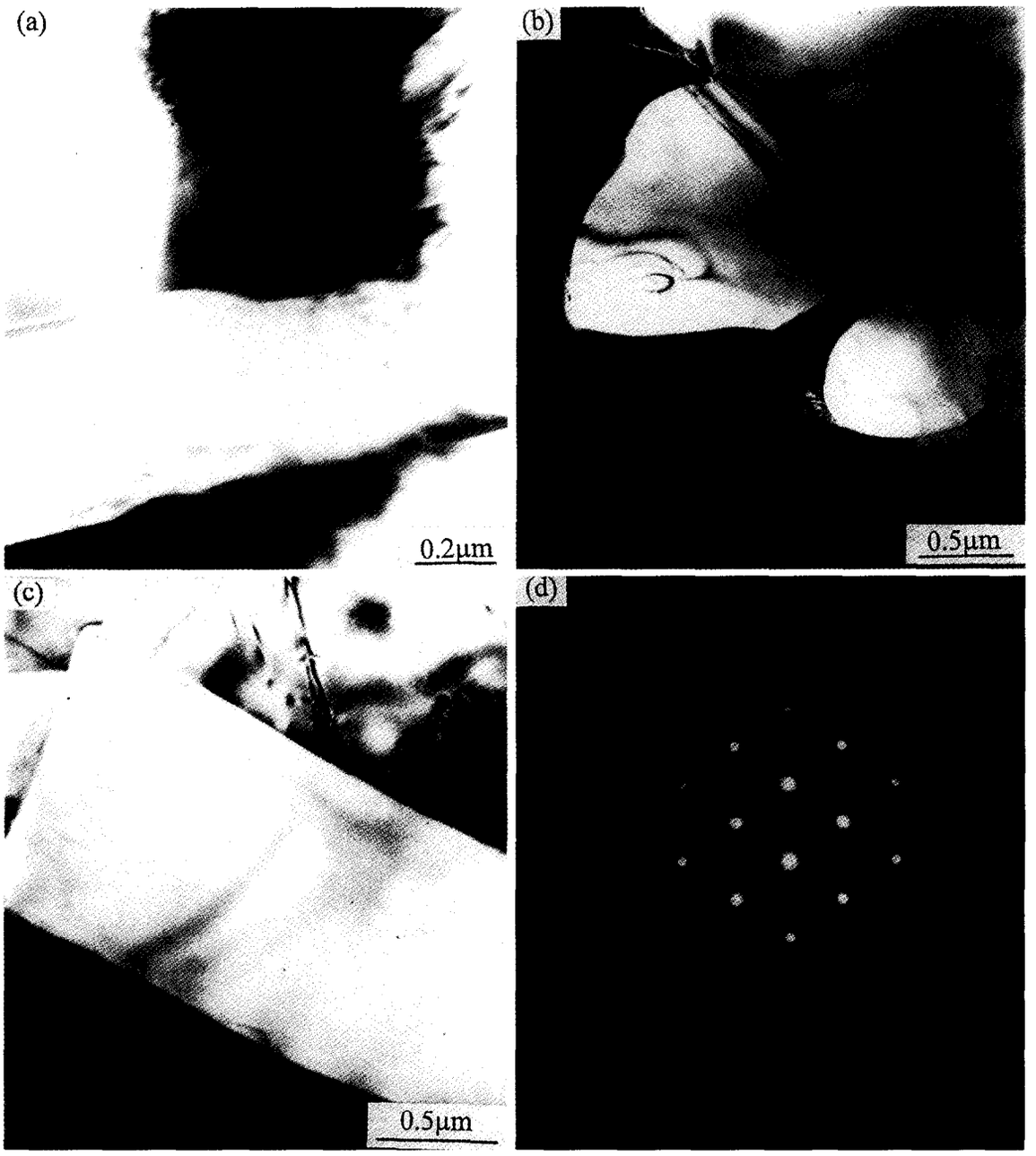

Fig. 3. TEM photographs showing the interfaces of SiCw/Al_2O_3 and SiCw/ZrO_2(2Y) in Al_2O_3+ZrO_2+SiCw composites. (a) AZS2 (Al_2O_3+20 vol% ZrO_2(2Y)+20 vol% SiCw), also showing the m-phase structure in ZrO_2(2Y) particles near the whiskers; (b), (c), AZS3 (Al_2O_3+20 vol% ZrO_2(2Y)+30 vol SiCw), also showing the microcracks and dislocations caused by the addition of SiCw; (d) diffraction pattern in (c) showing [011] zone of β-SiCw.

are Al_2O_3 grains. It can be found that SiCw and ZrO_2 particles are homogeneously dispersed in the Al_2O_3 matrix. SiCw is distributed in the grain boundaries of Al_2O_3 and ZrO_2 particles (Fig. 2(a)). However, a few of the small ZrO_2 grains are located in the Al_2O_3 grains. In addition most of the ZrO_2 grains are distributed in the grain boundaries of Al_2O_3 particles and SiCw. There are a number of dislocations in the Al_2O_3 grains near to the ZrO_2 grains, which were induced by the thermal incompatibility between the ZrO_2 and Al_2O_3 particles or the volume expansion caused by the t–m ZrO_2 phase transformation (Fig. 2(b) and (c)) so that the Al_2O_3 matrix can be strengthened by these small ZrO_2 grains. Sometimes the volume expansion can induce microcracks at the boundaries of Al_2O_3, ZrO_2 particles (Fig. 2(c) and (d)). A large number of TEM observations as shown in Fig. 3 indicate that most of the SiCw/Al_2O_3 and SiCw/ZrO_2 (2Y) interfaces are bonded tightly and there are no distinct second phases or intermediate layers formed at the interfaces, which is further demonstrated by the results of EDAX analysis (the diameter of electron beam is 2 nm) of the SiCw/Al_2O_3 and SiCw/ZrO_2 interfaces as shown in Fig. 4. There are no concentration gradients of Si, Al and Zr atoms. But some amount of (< 3 at%) Al and Zr atoms at the side of SiCw or Si atom at the sides of Al_2O_3

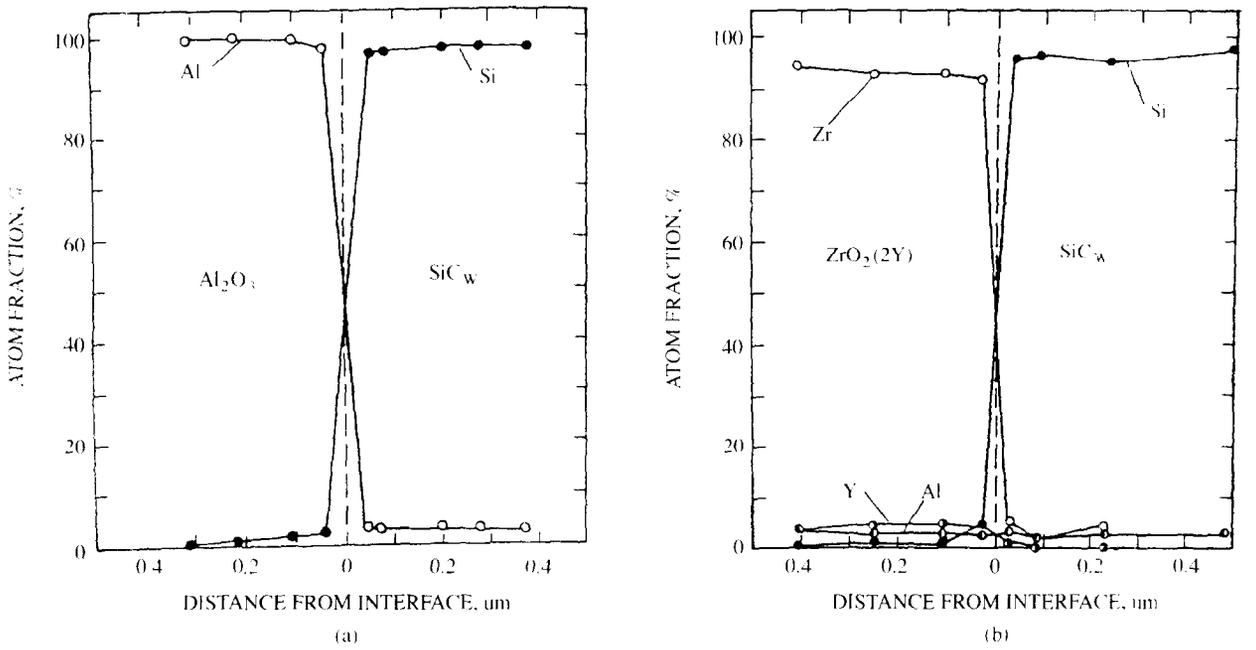

Fig. 4. Results of EDAX analysis of the $SiCw/Al_2O_3$ and $SiCw/ZrO_2(2Y)$ interfaces in $Al_2O_3 + ZrO_2(2Y) + SiCw$ composites. (a) $SiCw/Al_2O_3$ interface, (b) $SiCw/ZrO_2(2Y)$ interface.

and ZrO_2 (2Y) particles can be probed. This is caused by the ion sputtering during the preparation of TEM specimens. Figure 3(a) also shows that the t–m phase transformation can be enhanced by the tensile stresses in areas near the whiskers. Sometimes microcracks can be found at the $SiCw/Al_2O_3$ interfaces in the composites with higher SiCw contents (Fig. 3(b)). The dislocations in the Al_2O_3 grains could also be induced by the thermal incompatibility between SiCw and the Al_2O_3 matrix (as shown in Fig. 3(c)). A few defects such as stacking faults or twins can be seen in the cores of TWS-400 type of SiC whiskers. This is different from the observations given by Sarin[15] and Claussen.[4] The β-SiCw was rounded-triangular in cross section as shown in Fig. 3(b), which is confirmed by its diffraction pattern (Fig. 3(d)).

3.2 Mechanical properties

The Vicker's hardness and elastic modulus are obviously increased by the addition of SiCw as shown in Figs 5 and 6. A 30 vol% SiCw increases the hardness and the elastic modulus from 14.5 GPa and 401 GPa for the Al_2O_3 matrix to 18.6 GPa and 454 GPa, and 16.1 GPa and 380 GPa

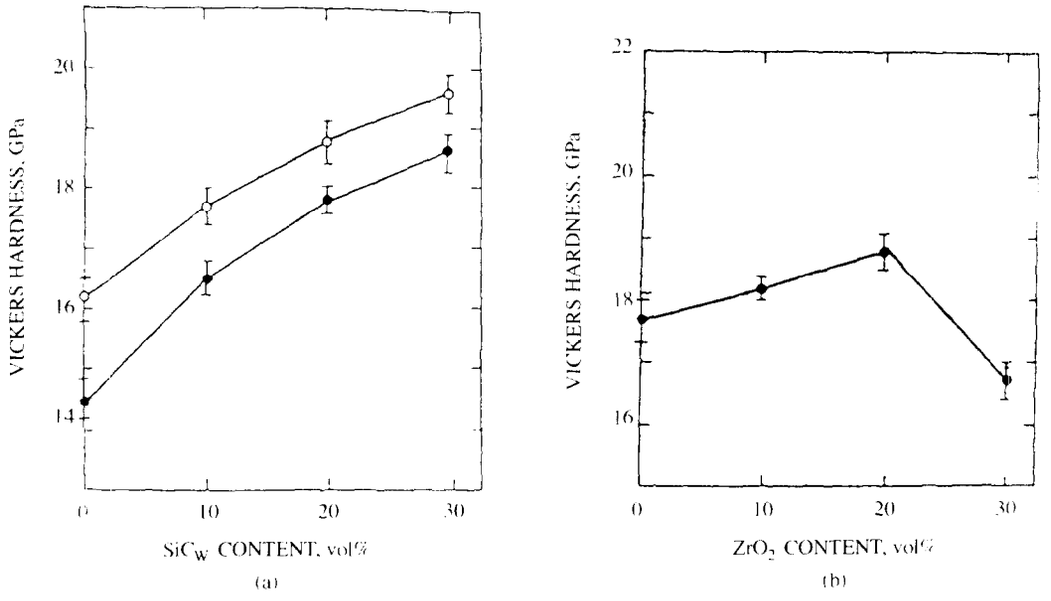

Fig. 5. Vickers hardness of AS, AZS and ASZ composites as functions of toughening phase content. (a) ● $AS(Al_2O_3 + SiCw)$, ○ $AZS(Al_2O_3 + 20\,vol\%\ ZrO_2(2Y) + SiCw)$; (b) $ASZ(Al_2O_3 + 20\,vol\%\ SiCw + ZrO_2(2Y))$.

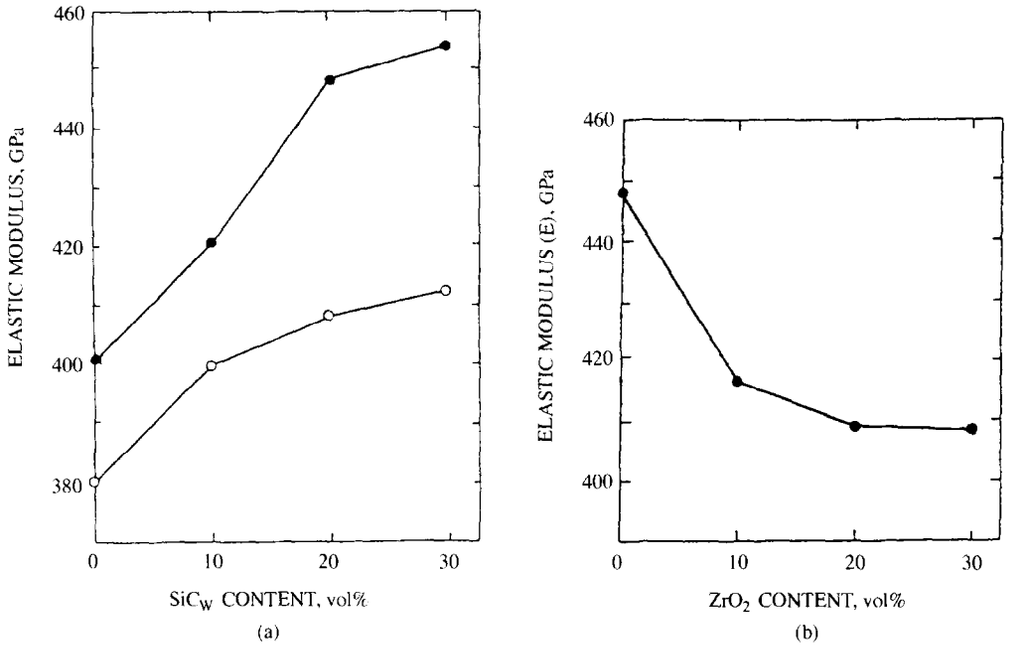

Fig. 6. Elastic modulus of AS, AZS and ASZ composites as functions of toughening phase content. (a) ●AS(Al_2O_3 + SiCw), ○ AZS(Al_2O_3 + 20 vol% ZrO_2(2Y) + SiCw); (b) ASZ(Al_2O_3 + 20 vol% SiCw + ZrO_2(2Y)).

for the Al_2O_3 + 20 vol% ZrO_2(2Y) matrix to 19.6 GPa and 413 GPa, respectively. The hardness value of AZS(Al_2O_3 + 20 vol% ZrO_2(2Y) + SiCw) composite is always higher than that of AS(Al_2O_3 + SiCw) composite with the same SiCw content, but its elastic modulus value is always lower than that of AS(Al_2O_3 + SiCw) composite. This is because that the addition of ZrO_2(2Y) component with a much lower modulus value (220 GPa) can refine the Al_2O_3 matrix and improve the densification of the AZS(Al_2O_3 + 20 vol% ZrO_2(2Y) + SiCw) composite. That is also the reason why the elastic modulus of ASZ(Al_2O_3 + 20 vol% SiCw + ZrO_2(2Y)) composite is clearly decreased by adding ZrO_2(2Y) particles and its hardness can be improved by the first adding 20 vol% ZrO_2(2Y) particles, then decreased by the further increment of the ZrO_2(2Y) particles content (as shown in Figs 5(b) and 6(b)).

The room temperature flexural strength and fracture toughness of these three series of composites are shown in Figs 7 and 8. The strength data

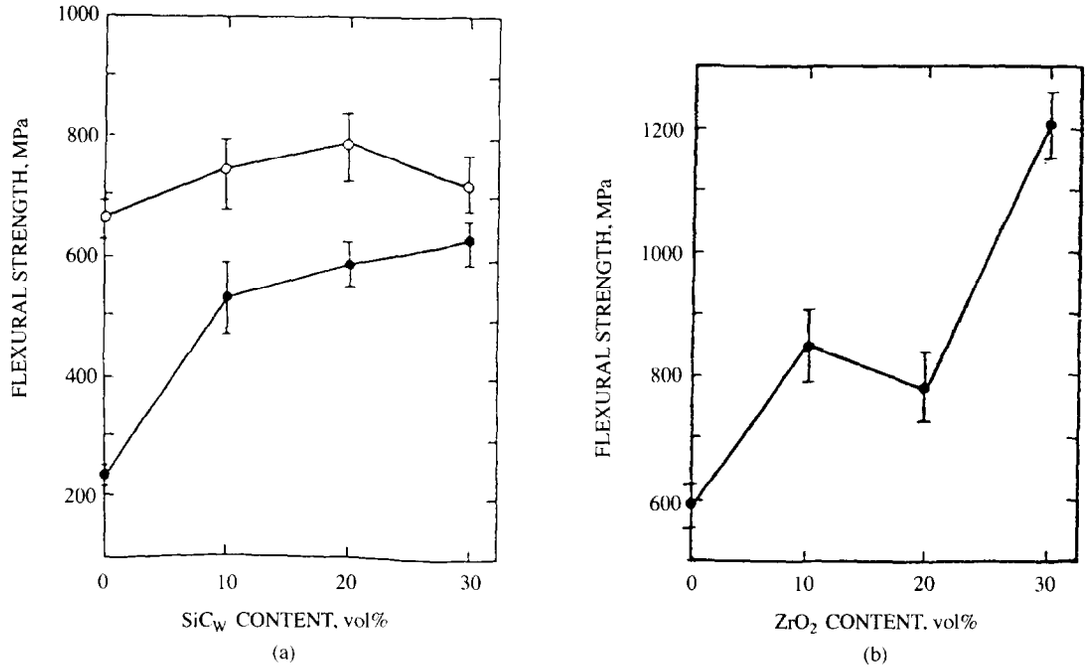

Fig. 7. Room temperature flexural strength of AS, AZS and ASZ composites as functions of toughening phase content. (a) ● AS(Al_2O_3 + SiCw), ○ AZS(Al_2O_3 + 20 vol% ZrO_2(2Y) + SiCw); (b) ASZ(Al_2O_3 + 20 vol% SiCw + ZrO_2(2Y)).

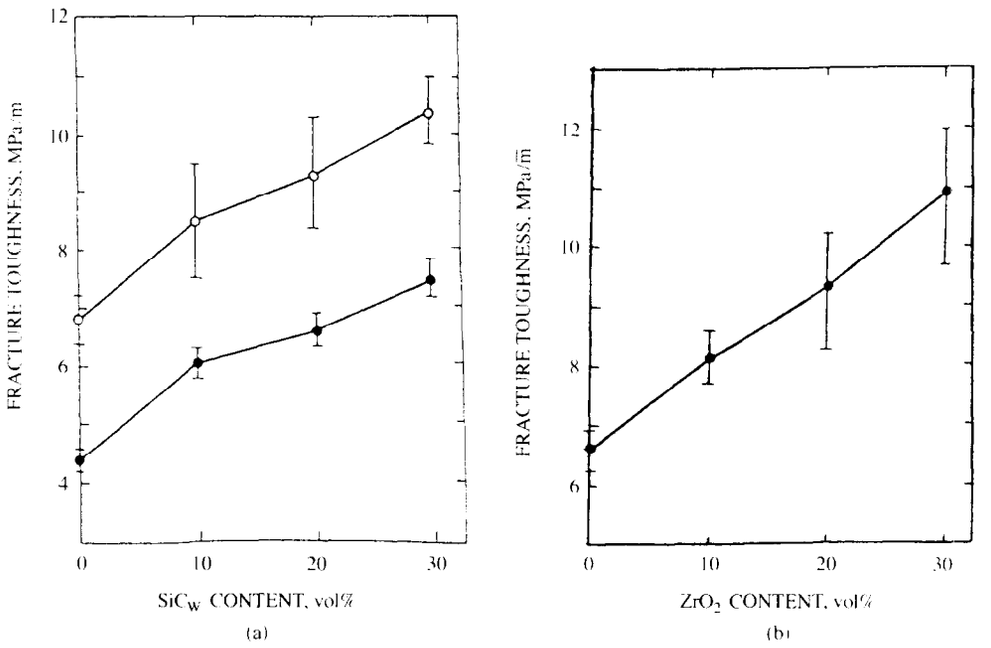

Fig. 8. Fracture toughness of AS, AZS and ASZ composites as functions of toughening phase conent. (a) ● AS(Al_2O_3 + SiCw), ○ AZS(Al_2O_3 + 20 vol% ZrO_2(2Y) + SiCw); (b) ASZ (Al_2O_3 + 20 vol% SiCw + ZrO_2(2Y)).

of the AS(Al_2O_3 + SiCw) series shown in Fig. 7(a) are very close to those obtained by Tiegs and Becher in 1987[8] and Yang and Stevens in 1991.[16] The first 10 vol% SiCw has very high strengthening effect and increases the flexural strength from 235 MPa for the matrix to 535 MPa. Further increment of the SiCw content leads to a much lower strengthening effect and the strength of Al_2O_3 + 30 vol% SiCw composite is only 634 MPa. The addition of 20 vol% ZrO_2(2Y) particles to Al_2O_3 matrix enormously increases the flexural strength to a value of 659 MPa, while the addition of SiCw increases only slightly the flexural strength of the AZS(Al_2O_3 + 20 vol% ZrO_2(2Y) + SiCw) series of composites with a maximum value of 784 MPa at 20 vol% SiCw. The further increment of the SiCw content leads, on the other hand, to a decrease in strength (720 MPa at 30 vol% SiCw). In ASZ(Al_2O_3 + 20 vol% SiCw + ZrO_2(2Y)) composites as shown in Fig. 7(b), the first 10 vol% ZrO_2(2Y) particles can obviously further improve the flexural strength from 592 MPa for the ASZ0 (AS2(Al_2O_3 + 20 vol% SiCw)) composite to 848 MPa. But the strength of ASZ2(Al_2O_3 + 20 vol% SiCw + 20 vol% ZrO_2(2Y)) composite is lower than that of ASZl(Al_2O_3 + 20 vol% SiCw + 10 vol% ZrO_2(2Y)) composite, while it is still much higher than that of ASZ0 composite. The flexural strength of ASZ3(Al_2O_3 + 20 vol% SiCw + 30 vol% ZrO_2(2Y)) composite is up to 1207 MPa, which is one times higher than that of ASZ0 composite. The decrease in strength in AZS(Al_2O_3 + 20 vol% ZrO_2(2Y) + SiCw) composites can be explained as a result of the formation of microcracks due to the thermal incompatibility between the Al_2O_3 and ZrO_2 particles with the SiCw and the t–m phase transformation (as shown in Figs 2(d) and 3(b).

It can be seen from Fig. 8 that the addition of 20 vol% ZrO_2(2Y) particles increases the fracture toughness of Al_2O_3 from its original value of 4.4 MPa$\sqrt{m}$ to 6.8 MPa$\sqrt{m}$. The addition of SiCw or ZrO_2(2Y) particles monotonically increases the fracture toughness of AS(Al_2O_3 + SiCw) and AZS(Al_2O_3 + 20 vol% ZrO_2(2Y) + SiCw) or ASZ(Al_2O_3 + 20 vol% SiCw + ZrO_2(2Y)) series of composites. A 30 vol% SiCw can increase the toughness of Al_2O_3 to 7.5 MPa$\sqrt{m}$ and the toughness of Al_2O_3 + 20 vol% ZrO_2(2Y)(AZS0) to 10.4 MPa$\sqrt{m}$, a 30 vol% ZrO_2(2Y) particles can increase the toughness of AS2(Al_2O_3 + 20 vol% SiCw) composite to 10.9 MPa$\sqrt{m}$. Obviously, additivity exists in the toughness effect of both SiCw and the ZrO_2 component for the Al_2O_3 matrix, but there is no additivity with respect to the strengthening effect. A part of this section has been published in literature.[17]

The flexural strength of some of Al_2O_3 + ZrO_2 + SiCw composites testing under air at 1000°C are summarized in Table 2. It is shown that the flexural strength of all of the composites with ZrO_2(2Y) component are greatly decreased at 1000°C, and the decrease in strength is more in the composite with higher ZrO_2(2Y) particles content. The strength of ASZ0(Al_2O_3 + 20 vol% SiCw), ASZ2(Al_2O_3 + 20 vol% SiCw + 20 vol% ZrO_2(2Y)) and ASZ3(Al_2O_3 + 20 vol% SiCw + 30 vol% ZrO_2(2Y)) composites with the same SiCw content (20 vol%) is almost the same at this time, which is

Table 2. Flexural strength of Al_2O_3+ZrO_2+SiCw composites at room temperature and 1000°C (MPa)

Composite	AZS0	AZS2	AZS3	ASZ0	ASZ3
Room temperature	659±34	784±56	720±53	592±34	1207±59
1000°C	375±40	463±27	578±31	483±33	502±52

independent of the ZrO_2(2Y) particles content. The strength of AZS(Al_2O_3 + 20 vol% ZrO_2(2Y) + SiCw) composites (AZS0(Al_2O_3 + 20 vol% ZrO_2(2Y)), AZS2(Al_2O_3 + 20 vol% ZrO_2(2Y) + 20 vol% SiCw) and AZS3(Al_2O_3 + 20 vol% ZrO_2(2Y) + 30 vol% SiCw)) are monotonically increased with the increment of SiCw content, a 30 vol% SiCw can increase the strength from 375 MPa for Al_2O_3 + 20 vol% ZrO_2(2Y) (AZS0) to 578 MPa at 1000°C, although the strength of AZS(Al_2O_3 + 20 vol% ZrO_2(2Y) + SiCw) composite reached a maximum value at 20 vol% SiCw at room temperature. Therefore, SiCw can still play a obvious role in strengthening Al_2O_3 matrix at high temperatures.

The substantial improvement in flexural strength (σ_f) and fracture toughness (K_{IC}) of the composites due to the addition of SiCw and ZrO_2(2Y) particles can be explained as follows. Firstly, there are strengthening and toughening effects of SiCw in the composites. The strengthening effect of SiCw can be performed by the load transferring effect if the whiskers and the matrix are bonded tightly since SiCw whiskers have high elastic modulus and high strength, and the strengthening effect can also be obtained by the refinement of the matrix grains (Fig. 9), the inhibition of the main crack propagation and in some cases the SiCw may directly join the rupture processes during the main crack propagation (Fig. 10). On the other hand, the addition of SiCw also has harmful effects on the flexural strength of the composites due to the high residual stresses caused by the thermal incompatibility between the SiC whiskers and the Al_2O_3, ZrO_2

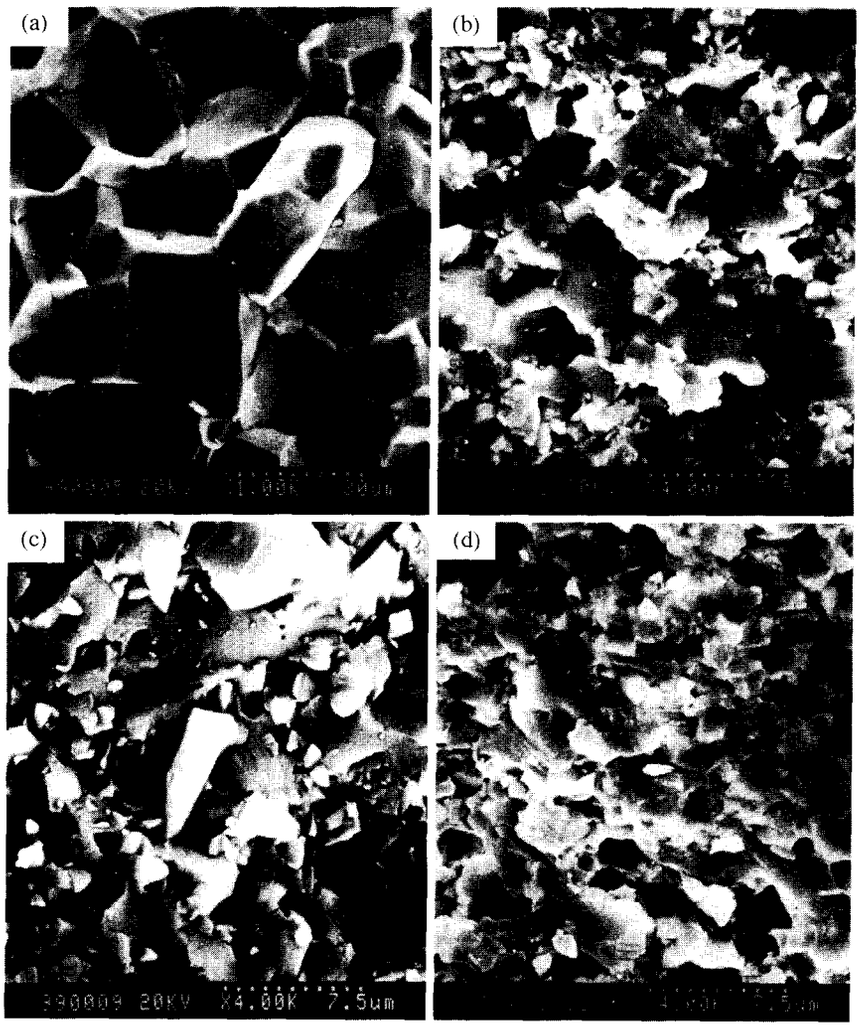

Fig. 9. SEM photographs of fractured surfaces of Al_2O_3 + ZrO_2 + SiCw composites bending at room temperature. (a) Al_2O_3; (b) Al_2O_3 + 20 vol% ZrO_2(2Y); (c) Al_2O_3 + 20 vol% SiCw; (d) Al_2O_3 + 20 vol% ZrO_2(2Y) + 20 vol% SiCw.

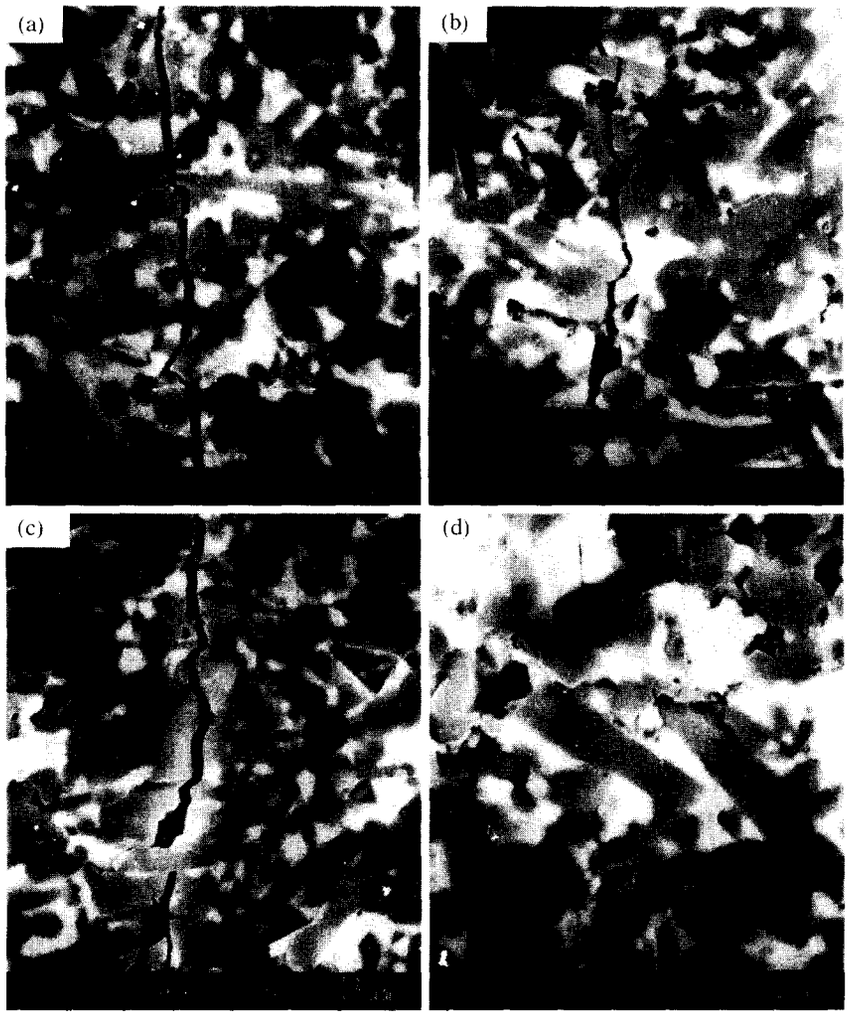

Fig. 10. SEM photographs of indentation crack propagation paths in $Al_2O_3 + 20$ vol% $ZrO_2(2Y) + 30$ vol% SiCw composite.

matrices, and the possibility of SiCw agglomeration becomes larger as the SiCw content increases and the critical defect size in the composites grows (Fig. 3(b)), resulting in the reduction of flexural strength. The toughening mechanisms of SiCw can be clearly demonstrated in the SEM photographs of the fractured surfaces of specimens for testing fracture toughness (Fig. 9) and the crack propagation paths at the corners of indents during hardness tests (Fig. 10). It can be seen that the addition of SiCw significantly refines the grain size of the Al_2O_3 matrix and changes the fracture mode from intergranular to preferentially transgranular. The microholes are left due to the pull-out of whiskers, and the roughness of the fractured surfaces is distinctly increased by the addition of whiskers. This is clear evidence of crack deflection so that more energy is absorbed during fracture of the SiCw containing materials. The crack deflection, SiCw rupture and SiCw pull-out and bridging are clearly seen in Fig. 10. These factors cause more energy consumption and improve the flexural strength and fracture toughness of the Al_2O_3 matrix. Secondly, there are strengthening and toughening effects of $ZrO_2(2Y)$ particles in the composites. The strengthening and toughening mechanisms of $ZrO_2(2Y)$ particles include several following aspects: The first is the dynamic t–m phase transformation toughening effect during fracturing revealed by X-ray analysis as shown in Table 3. The second is the microcrack toughening effect induced by the volume expansion caused by the t–m phase transformation during cooling from the hot-pressing temperature (Fig. 2(c) and (d)). Such microcracks may be harmful to the strengthening, as shown in Fig. 7 for the AZS($Al_2O_3 + 20$ vol% $ZrO_2(2Y) + SiCw$) composites. The third is the refinement of Al_2O_3 matrix grains with the addition of $ZrO_2(2Y)$ particles (Fig. 9) and strengthening effect on the Al_2O_3 matrix by dispersing in the Al_2O_3 grains (Fig. 2(b) and (c)). In addition, the ZrO_2 particles can effectively enhance the crack deflection and shield the main crack from further propagation (Fig. 10(d)). These factors result in the substantial higher flexural strength and fracture toughness of $Al_2O_3 + ZrO_2 + SiCw$ composites than that of AS($Al_2O_3 + SiCw$) composites.

Table 3. Amount of t–m phase transformation of ZrO_2 in Al_2O_3+ZrO_2+SiCw composites during fracture of SENB tests

Materials	AZS0	AZS1	AZS2	AZS3	ASZ0	ASZ1	ASZ2	ASZ3
Amount of m-phase on polished surface (%)	8.7	7.6	10.8	16.8	0	12.99	10.80	13.88
Amount of m-phase on fractured surface (%)	13.40	19.30	28.80	33.30	0	29.79	29.80	31.10
Amount of t–m transformation during fracture (%)	4.70	11.70	19.00	16.50	0	16.80	19.00	17.22

The addition of SiCw has twofold effects on the t–m phase transformation: on the one hand, the higher elastic modulus of SiCw and the refining effect on the $ZrO_2(2Y)$ particles inhibit the t–m phase transformation; on the other hand, the tensile stresses in the ZrO_2 particles induced by the thermal incompatibility between SiCw and the ZrO_2 grains and the toughening effect of SiCw enhance this transformation.[18] This is the reason that the amounts of t–m phase transformation in AZS (Al_2O_3 + 20 vol% $ZrO_2(2Y)$ + SiCw) composites gradually increase with increasing SiCw content and in ASZ(Al_2O_3 + 20 vol% SiCw + $ZrO_2(2Y)$) composites with the same SiCw content are almost the same, they are between 17–19%, as shown in Table 3. At the same time, the addition of $ZrO_2(2Y)$ particles has twofold effects on the strengthening and toughening effects of SiCw: the volume expansion caused by the t–m phase transformation during cooling from the sintering temperature can counteract part of the thermal stresses and improve the bonding strength of SiCw/matrix interface, which may be beneficial in the strengthening and toughening effects of SiCw; but the microcracks induced by the volume expansion are harmful to the strengthening effect of SiCw. It is the harmful effect of the addition of $ZrO_2(2Y)$ particles that causes that the increments in strength of Al_2O_3 + $ZrO_2(2Y)$ matrix are always lower than that of Al_2O_3 matrix with the same addition of SiCw and that the strength of ASZ2(Al_2O_3 + 20 vol% SiCw + 20 vol% $ZrO_2(2Y)$) composite is, on the contrary, lower than that of ASZ1(Al_2O_3 + 20 vol% SiCw + 10 vol% $ZrO_2(2Y)$). The obvious improvement in the strength of Al_2O_3 + 20 vol% SiCw composite with adding the first 10 vol% $ZrO_2(2Y)$ particles is due to the phase transformation toughening effect, refinement of Al_2O_3 matrix grains, decrease in the thermal stresses, improvements in the bonding strength of the interfaces and the densification of the composites, but at this time the less harmful effect because of the lower $ZrO_2(2Y)$ particles content. In ASZ3(Al_2O_3 + 20 vol% SiCw + 30 vol% $ZrO_2(2Y)$) composite, the possibilities of SiCw touching with $ZrO_2(2Y)$ particles directly and the agglomeration of $ZrO_2(2Y)$ particles become more intense so that the thermal stresses can be more effectively decreased, the bonding strength of SiCw/matrix interface is further improved and the possibility of the microcracks forming in the $Al_2O_3/ZrO_2(2Y)$ interfaces and $ZrO_2(2Y)$ ceramics with higher strength and toughness[19] increases so that the microcrack sizes can be obviously decreased (as shown in Fig. 2(d), compared with Fig. 2(c)). Therefore, the strength of ASZ3(Al_2O_3 + 20 vol% SiCw + 30 vol% $ZrO_2(2Y)$) composite is greatly improved. As shown in Fig. 8, the toughening effects of both SiCw and $ZrO_2(2Y)$ particles increase monotonically the fracture toughness values of AS(Al_2O_3 + SiCw), AZS(Al_2O_3 + 20 vol% $ZrO_2(2Y)$ + SiCw) and ASZ(Al_2O_3 + 20 vol% SiCw + ZrO_2 (2Y)) composites with the increment of SiCw or $ZrO_2(2Y)$ particles content and the improvement in the fracture toughness of Al_2O_3 matrix contributed by combining SiCw and $ZrO_2(2Y)$ particles is larger than the addition of the improvement contributed by one of the two toughening components.

3.3 Thermal shock behaviour

The flexural strength of AS(Al_2O_3 + SiCw), AZS(Al_2O_3 + 20 vol% $ZrO_2(2Y)$ + SiCw) and ASZ(Al_2O_3 + 20 vol% SiCw + $ZrO_2(2Y)$) series of composites before and after thermal shocking ($\Delta T = 800°C$) and the residual strength ratio as functions of toughening phase content are given in Fig. 11. Here σ_f is the flexural strength before thermal shocking, σ_R is the flexural strength after thermal shocking, σ_R/σ_f is the residual strength ratio. In order to compare with σ_R conveniently, the data of σ_f are also shown in Fig. 11. The addition of SiCw obviously improves the thermal shock resistance of Al_2O_3 and Al_2O_3 + $ZrO_2(2Y)$ ceramics (as shown in Fig. 11(a) and (b)). After thermal shocking with temperature difference up to 800°C, pure Al_2O_3 showed a significant decrease in flexural strength retained, the σ_R/σ_f value is only 60%, but ASl(Al_2O_3 + 10 vol% SiCw) and AS2(Al_2O_3 + 20 vol% SiCw) composites showed no decrease in flexural strength and AS3(Al_2O_3 + 30 vol% SiCw) composite showed only a slight decrease in strength, its σ_R/σ_f value is 96%. This result indicates that the critical temperature change (ΔTc) for strength degradation for the AS(Al_2O_3 + SiCw) composites is higher than

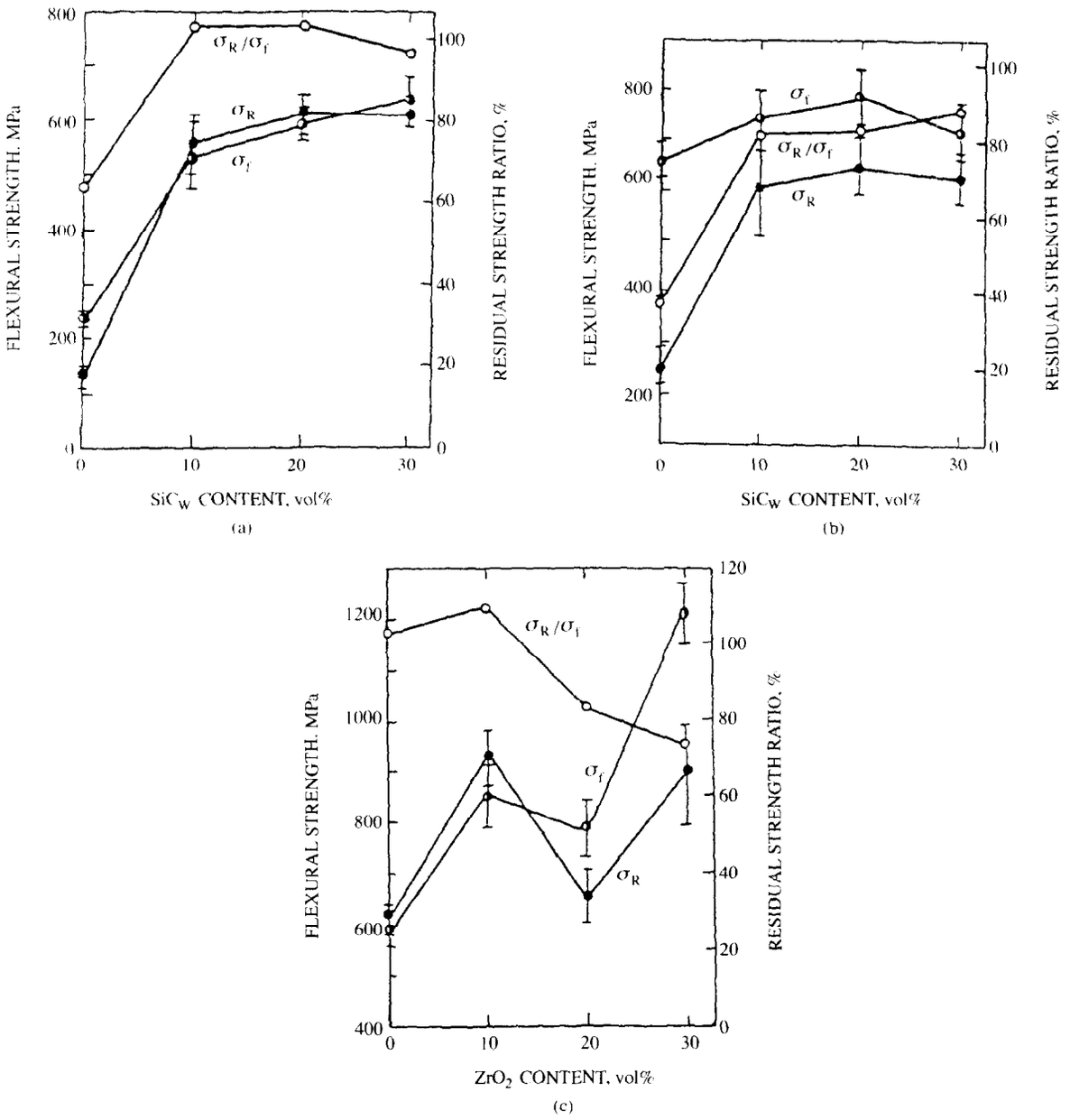

Fig. 11. Flexural strength of AS, AZS and ASZ composites before and after thermal shocking and the residual strength ratio as functions of toughening phase content ($\Delta T = 800°C$): (a) $AS(Al_2O_3 + SiCw)$; (b) $AZS(Al_2O_3 + 20\,vol\%\ ZrO_2(2Y) + SiCw)$; (c) $ASZ(Al_2O_3 + 20\,vol\%\ SiCw + ZrO_2(2Y))$. σ_f, flexural strength before thermal shocking; σ_R, flexural strength after thermal shocking; σ_R/σ_f, residual strength ratio.

800°C, which is consistent with the result of Tiegs and Becher in 1987.[20] The residual strength ratios of $AZS(Al_2O_3 + 20\,vol\%\ ZrO_2(2Y) + SiCw)$ composites are monotonocally increased with the increment of SiCw content although the σ_R of $AZS3(Al_2O_3 + 20\,vol\%\ ZrO_2(2Y) + 30\,vol\%\ SiCw)$ composite (635 MPa) is still slightly lower than that of $AZS2(Al_2O_3 + 20\,vol\%\ ZrO_2(2Y) + SiCw)$ (648 MPa). An addition of 30 vol% SiCw increases the σ_R/σ_f from 38% for $AZS0(Al_2O_3 + 20\,vol\%\ ZrO_2(2Y))$ composite to 88%. However, the residual strength ratios of $AZS(Al_2O_3 + 20\,vol\%\ ZrO_2(2Y) + SiCw)$ composites are distinctly lower than that of $AS(Al_2O_3 + SiCw)$ composites with the same SiCw content. It can be seen from Fig. 11(c) that the thermal shock resistance of $AS2(Al_2O_3 + 20\,vol\%\ SiCw)$ composite can be further improved by adding 10 vol% $ZrO_2(2Y)$ particles. Further increment of $ZrO_2(2Y)$ particles content (more than 20 vol%), on the other hand, seriously decreases the thermal shock resistance of $ASZ(Al_2O_3 + 20\,vol\%\ SiCw + ZrO_2(2Y))$ composites. The σ_R/σ_f values of $ASZ2(Al_2O_3 + 20\,vol\%\ SiCw + 20\,vol\%\ ZrO_2(2Y))$ and $ASZ3(Al_2O_3 + 20\,vol\%\ SiCw + 30\,vol\%\ ZrO_2(2Y))$ composites are only 83% and 74%, respectively.

The improvement in the thermal shock resistance of the Al_2O_3 and $Al_2O_3 + ZrO_2$ ceramics by adding SiCw is believed to be due to: (1) the addition of SiCw obviously increased the fracture toughness of

AS(Al_2O_3 + SiCw) and AZS(Al_2O_3 + 20 vol% ZrO_2(2Y) + SiCw) composites so that the thermal shock microcracks were impeded to coalesce into large cracks by whisker pinning or bridging; (2) the σ_f/E ratios of AS(Al_2O_3 + SiCw) and AZS(Al_2O_3 + 20 vol% ZrO_2(2Y) + SiCw) composites were increased by the addition of SiCw so that the nucleation energy of the thermal shock microcracks in the composites was increased; and (3) the thermal conductivity became higher and the thermal expansion became lower for AS(Al_2O_3 + SiCw) and AZS(Al_2O_3 + 20 vol% ZrO_2(2Y) + SiCw) composites with adding SiCw so that the thermal stress was decreased in the composites during thermal shocking and the thermal shock resistance of the composites was further improved. The results shown in Fig. 11(c) for ASZ(Al_2O_3 + 20 vol% SiCw + ZrO_2(2Y)) series of composites can be understood as follows: the thermal stress in the Al_2O_3 + ZrO_2(2Y) matrix can be partially counteracted by the volume expansion caused by the t–m phase transformation during quenching with adding 10 vol% ZrO_2(2Y) particles and the bonding strength of the SiCw/matrix interface was increased so that the strengthening effect of SiCw was improved. In addition, the Al_2O_3 grains were obviously further refined by adding ZrO_2(2Y) particles. These favourable factors greatly improved the thermal shock resistance of ASZ(Al_2O_3 + 20 vol% SiCw + ZrO_2(2Y)) composites. It can be seen from the fracture surfaces as shown in Fig. 12 (c) that the matrix grains and SiCw/matrix interfaces are also bonded tightly after thermal shocking. However, higher ZrO_2(2Y) particle contents (20, 30 vol%) might cause larger t–m phase transformation during quenching so that the microcracks might coalesce into large danger cracks and the SiCw/matrix interfaces were debonded (as shown in Fig. 12(a), (b) and (d) and the thermal shock resistance of ZrO_2(2Y) ceramics is lower. These unfavourable factors greatly decreased the thermal shock resistance of Al_2O_3 + ZrO_2 + SiCw composites and the σ_R/σ_f values of

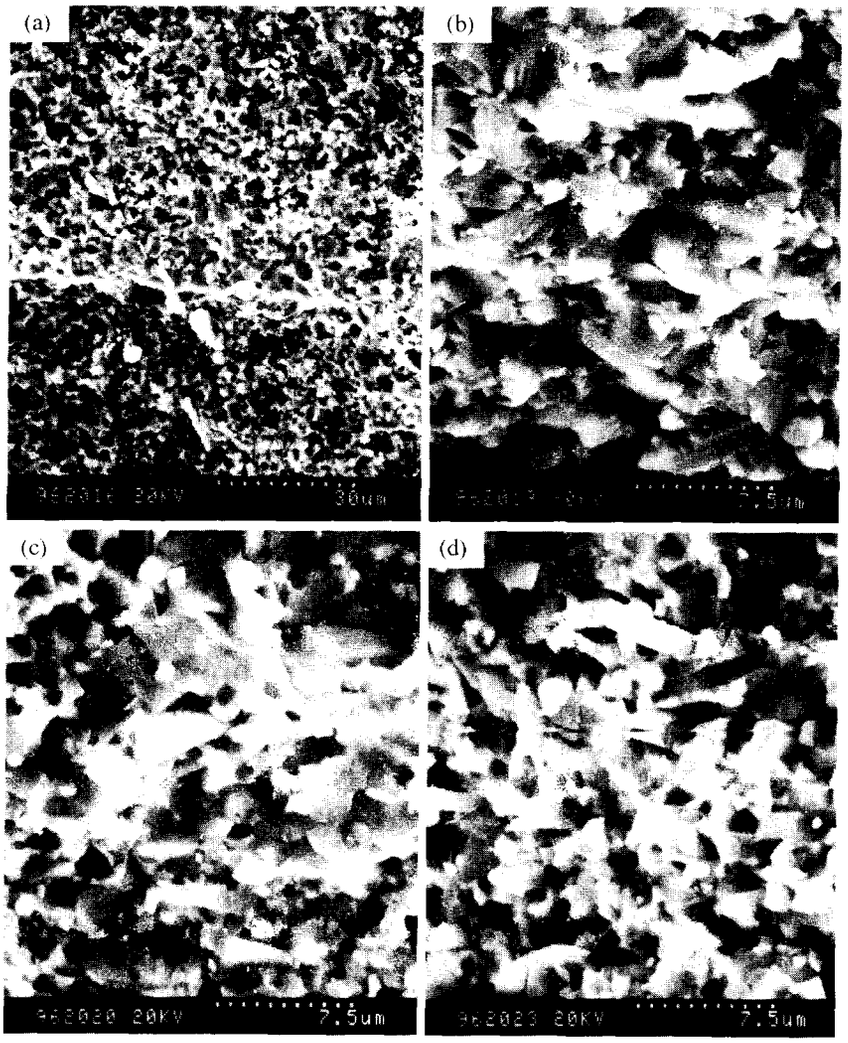

Fig. 12. SEM photographs of bending fractured surfaces of Al_2O_3 + ZrO_2 + SiCw composites after thermal shocking ($\Delta T = 800°C$). (a) AZS0 (Al_2O_3 + 20 vol% ZrO_2(2Y)); (b) AZS3 (Al_2O_3 + 20 vol% ZrO_2(2Y) + 30 vol% SiCw); (c) ASZ1 (Al_2O_3 + 20 vol% SiCw + 10 vol% ZrO_2(2Y)); (d) ASZ3 (Al_2O_3 + 20 vol% SiCw + 30 vol% ZrO_2(2Y)).

ASZ2(Al_2O_3 + 20 vol% SiCw + 20 vol% ZrO_2(2Y)) and ASZ3(Al_2O_3 + 20 vol% SiCw + 30 vol% ZrO_2(2Y)) composites so that the σ_R/σ_f values of AZS(Al_2O_3 + 20 vol% ZrO_2(2Y) + SiCw) composites are much lower than that of AS(Al_2O_3 + SiCw) composites with the same SiCw contents. Therefore, no too much ZrO_2(2Y) particles should be added to $Al_2O_3 + ZrO_2$ + SiCw composites on behalf of improving the thermal shock resistance of the composites.

4 CONCLUSIONS

1. SiCw and ZrO_2(2Y) particles are homogeneously dispersed in the Al_2O_3 matrix. $Al_2O_3 - ZrO_2$ + SiCw composites can be sintered to a high densification by hot-pressing. The addition of proper amounts of ZrO_2(2Y) particles ($\leq$20 vol%) can effectively improve the densification of Al_2O_3 + SiCw composites. The addition of SiCw or ZrO_2(2Y) particles significantly refines the size of the Al_2O_3 matrix grains.
2. Most of the SiCw/Al_2O_3 and SiCw/ZrO_2(2Y) interfaces are bonded tightly and no distinct second phases or intermediate layers can be observed at the interfaces under analytical TEM. The crystal structure of TWS-400 type of SiCw is more perfect and is face centered cubic lattice. Its cross-section is rounded triangular.
3. The addition of SiCw or ZrO_2(2Y) particles substantially improve the flexural strength and fracture toughness of Al_2O_3 ceramics. The more obvious strengthening and toughening effects can be obtained by adding both SiCw and ZrO_2(2Y) particles simultaneously to the Al_2O_3 matrix. The flexural strength and fracture toughness of Al_2O_3 + 20 vol% SiCw + 30 vol% ZrO_2(2Y) composite at room temperature are 1207 MPa and 10.9 MPa$\sqrt{m}$, respectively. SiCw also has obvious strengthening effect on Al_2O_3 and $Al_2O_3 + ZrO_2$ ceramics composites at 1000°C.
4. The main toughening mechanisms in the $Al_2O_3 + ZrO_2$ + SiCw composites are whisker bridging and pull-out, crack deflection as well as dynamic t-m phase transformation toughening and microcrack toughening. The contribution of combining both SiCw reinforcing and ZrO_2(2Y) phase transformation toughening to the fracture toughness of Al_2O_3 matrix is larger than the addition of the contribution obtained by using one of the two toughening components individually. But the microcracks induced by the t–m phase transformation and the thermal stresses are harmful to the strengthening effect of SiCw.
5. The high elastic modulus of SiCw and Al_2O_3 and the refining effect on the ZrO_2(2Y) particles inhibit the t–m ZrO_2 phase transformation; The tensile stresses in the ZrO_2(2Y) grains induced by the thermal incompatibility between SiCw and ZrO_2 and the toughening effect of SiCw enhance this transformation.
6. The addition of SiCw can obviously improve the thermal shock resistance of Al_2O_3 and $Al_2O_3 + ZrO_2$(2Y) ceramics. The addition of a few of ZrO_2(2Y) particles (10 vol%) can further improve the thermal shock resistance of Al_2O_3 + SiCw composites. But further increment of ZrO_2(2Y) particles content ($\geq$20 vol%) seriously decreases the thermal shock resistance of $Al_2O_3 + ZrO_2$ + SiCw composites because of a number of microcracks caused by the t–m phase transformation during quenching.

REFERENCES

1. LANGE, F. F., Transformation toughening, Part 2: Contribution to fracture toughness. *J. Mater. Sci.*, **17** (1982) 235–239.
2. CLAUSSEN, N., Fracture toughness of Al_2O_3 with an unstabilized ZrO_2 dispersed phase. *J. Am. Ceram. Soc.*, **59**(1) (1976) 49–51.
3. TIEGS, T. N. & BECHER, P. F., Whisker reinforced ceramics composites. *Mater. Sci. Res.*, **20** (1986) 639–647.
4. CLAUSSEN, N., WEISSKOPF, K. L. & RÜHLE, M., Tetragonal zirconia polycrystal reinforced with SiC whiskers. *J. Am. Ceram. Soc.*, **69**(3) (1986) 288–292.
5. BECHER, P. F., Toughening behavior in ceramics associated with the transformation of tetragonal ZrO_2. *Acta Metall.*, **3**(10) (1986) 1885–1891.
6. BECHER, P. F. & TIEGS, T. N., Temperature dependence of strengthening by whisker reinforcement: SiC whisker reinforced alumina in air. *Adv. Ceram. Mater.*, **3**(2) (1988) 148–153.
7. BECHER, P. F., TIEGS, T. N., OGLE, J. C. & WARWICK, W. H., Toughening of ceramics by whisker reinforcement, in *Fracture Mechanics of Ceramics, Vol. 7*, ed. by R. C. Bradt, Plenum Press, New York, 1986, pp. 61–73.
8. TIEGS, T. N. & BECHER, P. F., Sintered Al_2O_3–SiC whisker composites. *Am. Ceram. Soc. Bull.*, **66**(2) (1987) 339–342.
9. CLAUSSEN, N. & PETZOW, G., Whisker-reinforced zirconia-toughened ceramics. *Mater. Sci. Res.*, **20** (1986) 649–662.
10. CLAUSSEN, N. & SWAIN, M. V., Silicon carbide whisker reinforced and zirconia transformation toughened ceramics. *Mater. Forum*, **11** (1988) 194–201.
11. BOHMER, M. & ALMOND, E. A., Mechanical properties and wear resistance of a whisker-reinforced zirconia-toughened alumina. *Mater. Sci. Eng.*, **A105/106** (1988) 105–116.
12. SOLOMAH, A. C. & REICHERT, W., Mechanical properties, thermal shock resistance and thermal stability of zirconia-toughened alumina–10 vol% silicon carbide whisker ceramic matrix composite. *J. Am. Ceram. Soc.*, **73**(3) (1990) 740–743.

13. CALES, B., MATHIEU, P. & TORRE, J. P., Preparation and characterization of whisker reinforced zirconia toughened alumina, in *Science of Ceramics 14*, ed. D. Taylor. The Institute of Ceramics, Stoke-on-Trent, UK, 1988, pp. 813–818.
14. WEI, G. C. & BECHER, P. F., Development of SiC whisker reinforced ceramics.. *Am. Ceram. Soc. Bull.*, **64**(2) (1985) 298–304.
15. SARIN, V. K. & RÜHLE, M., Microstructural studies of ceramic matrix composites,. *Composites*, **18**(2) (1987) 129–134.
16. YANG, M. & STEVENS, R., Microstructure and properties of SiC whisker reinforced ceramic composites. *J. Mater. Sci.*, **26** (1991) 726–736.
17. LIN, G. Y., LEI, T. C., ZHOU, Y. & WANG, S. X., Mechanical properties of Al_2O_3 and $Al_2O_3 + ZrO_2$ ceramics reinforced by SiC whiskers. *J. Mater. Sci.*, **28** (1993) 2745–2749.
18. LIN, G. Y., LEI, T. C. & ZHOU, Y., Effects of SiC whiskers on the t–m ZrO_2 phase transformation in ceramic matrix composites. *J. Mater. Sci. Lett.*, **15**(14) (1996) 1267–1270.
19. LIN, G. Y., LEI, T. C., WANG, S. X. & ZHOU, Y., Microstructure and mechanical properties of SiC whisker reinforced ZrO_2(2 mol% Y_2O_3) based composites. *Ceram. Int.*, **22**(3) (1996) 199–205.
20. TIEGS, T. N. & BECHER, P. F., Thermal shock behavior of an alumina–SiC whisker composite. *J. Am. Ceram. Soc.*, **70**(5) (1987) C109.